First International Symposium on Marine Propulsors
smp'09, Trondheim, Norway, June 2009

Comparison of hydrodynamics performances of a porpoising foil and a propeller

France Floc'h[1], **Jean Marc Laurens**[1] **and Jean Baptiste Leroux**[1]

[1]Laboratoire Brestois de Mécanique et des Systèmes (LBMS), EA4325, ENSIETA, Brest, France

ABSTRACT

A numerical method involving an Euler-Newton equations solver and the equations of hydrodynamics has been developed. This method is used to simulate biomimetic propulsion by a porpoising foil. To compare the hydrodynamic performances of a porpoising foil with a conventional fixed pitch propeller, all degrees of freedom are fixed. The hydrodynamic solver is a potential flow code. It is used for the two propulsion devices which makes simulations easy and fast. The thrust produced by porpoising foils is studied numerically. The parametric study confirms that the multiplicative inverse of the Strouhal number is playing the same role for the oscillating wing, the advance parameter is playing for the propeller. A porpoising rigid foil will present an efficiency curve comparable to the one of a propeller as long as its motion is regular. The angle of pitch and the heave amplitude of the motion have to be regarded as geometric parameters comparable to the propeller pitch. Our results for the thrust coefficient are in conformity with the Theodorsen theory over the whole range of parameters. The porpoising foil hydrodynamic performances are then compared with those of a propeller. Finally unsteady state simulations comparative results are also presented, the propeller pitch variation being analogous to a change in the foil motion.

Keywords

propulsion, hydrofoil, porpoising, biomimetism

1 INTRODUCTION

Porpoising foils have been extensively studied because they consist of a simple model to understand fish and cetacean propulsion. A leader in this subject is M.S. Triantafyllou who has spent the last decade publishing on it. Its work began on the physics of the problem with vorticity consideration (Streitlien et al., 1996; Triantafyllou et al., 2000), and evolves to the study of hydrodynamic performances (Schouveiler et al., 2005). Such motions are studied also in (Barrett et al., 1999), (Guglielmini and Blondeaux, 2004) and (Pedro et al., 2003). These articles deal with the lift due to vortex generation and the characteristics of the motion like the tail form and the animals Strouhal number which ranges from 0.2 to 0.4 for fish and cetacean. Nevertheless, real industrial applications exist such as cycloidal propellers (Jurgens (2001)).

In the first part, the numerical method and the simulations are described. The method is verified by simulating a natural decrease of speed of a foil due to drag force. The analytical solution for speed is detailed. In the second part, the Theodorsen theory is applied to a porpoising NACA0012 foil. Then the hydrodynamic performances results for a foil are defined and computed and then compared to the performances of a propeller. The pitch variation case is described at the end of the last part.

2 NUMERICAL METHOD

In order to compute the trajectory and the forces acting on the foil, an unsteady potential flow code is used coupled with a Euler-Newton equations solver.

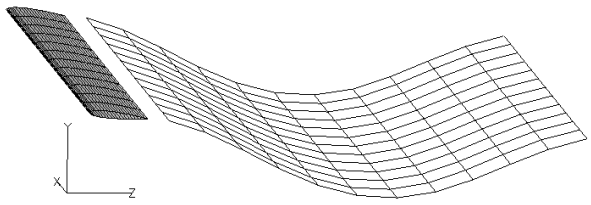

Figure 1: Panels used by the potential flow code

The potential flow code is a Boundary Element Method (BEM) code. It belongs to what Hoeijmakers (1991) refers as "second generation" panel methods involving the Dirichlet condition. Body surfaces are discretised into first order panels carrying constant source and doublet distributions. The wake developing behind the foil (see figure 1) is formed with a sheet of first order panels carrying constant doublet distributions and it is generated with time in a Lagrangian manner. It is legitimate to use a potential flow code considering that in all our simulations, lifting bodies are used with $Re \geq 10^6$ and the angle of attack with the current remains small at all time. The friction is also taken into account. The code modifies the friction coefficient with the local Reynolds number: $Re(x) = V(x)(x-x_0)/\nu$ with x_0 at the leading edge. If $Re(x) < 5.10^5$, the flow is supposed laminar and $C_f(x) = \dfrac{0.664}{\sqrt{Re(x)}}$, else the flow

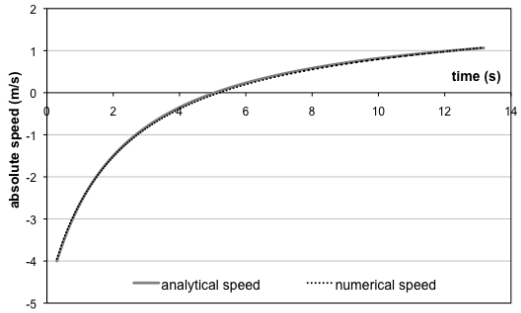

Figure 2: Comparison between analytical and coupling codes results for a natural decreasing speed

is supposed turbulent and $C_f(x) = \dfrac{0.027}{\sqrt[7]{Re^*(x)}}$, $Re^*(x) = V(x)(x - x_t)/\nu$ with x_t, the transition position. This code is coupled with a routine solving the equations of motion. From the forces integrated on the panels, the routine calculated the new velocities and position of the center of gravity. The numerical method used is a Crank-Nicholson scheme. Its stability is discussed in Floc'h et al. (2008). A preliminary study has permitted to define the mesh and time steps refinement range applicable to avoid discretization sensibility.

3 VERIFICATION

3.1 Preliminary

To verify our method, a wing with NACA 23012 section presenting an angle of attack of 6°, a chord of 1 m, a span of 3 m and an initial speed of 4 m/s is placed in an invert flow of 2 m/s. From this initial state, a natural decreasing speed due to drag is simulated. This speed is compared to an analytical speed on the figure 2.

The analytical speed is calculated by solving the second law of Newton:

$$(m + m_a)\frac{\partial v}{\partial t} = \frac{1}{2}\rho C_D S(v(t) - U_\infty)^2 \qquad (1)$$

with m, the mass of the foil; m_a, its added mass; S its planform area; C_D, its drag coefficient and ρ, the fluid density. The velocity is thus:

$$v(t) = \frac{1}{(v_0 - U_\infty)^{-1} - \beta t} + U_\infty \qquad (2)$$

with $\beta = \dfrac{\rho C_D S}{2(m + m_a)}$ and v_0 the initial speed. The lift coefficient, C_l, is referenced in Abbott and Von Doenhoff (1959): for a NACA 23012 with an attack angle 6° and a Reynolds number close to one million, is 0.75. The profile aspect ratio is $\Lambda = 3$. According to the Hembold formula:

$$C_L = C_l \times \frac{\Lambda}{\sqrt{\Lambda^2 + 4} + 2}$$

and considering a 3D problem, C_D is thus:

$$C_D = \frac{C_L^2}{\pi\Lambda} = 0.04 \qquad (3)$$

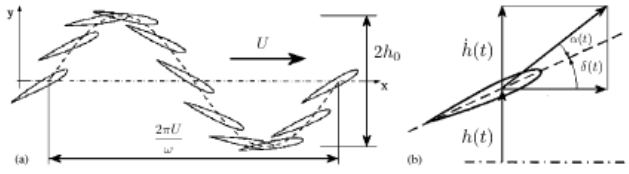

Figure 3: (a) Kinematical parameters of the foil motion and (b) definition of the effective angle of attack $\alpha(t)$, from Guglielmini et al. (2004)

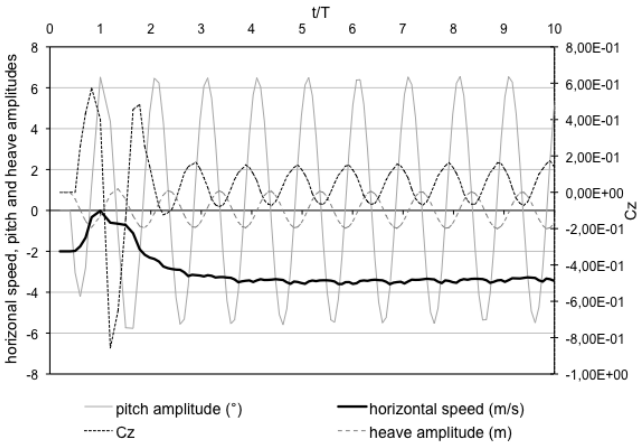

Figure 4: Characteristics of the motion

In order to obtain the added mass m_a, potential flow simulations with constant acceleration have been previously performed. The results, plotted on figure 2, are, as expected, almost similar.

3.2 Free Oscillating Foil

As mentioned in the introduction, the hydrodynamic performances of a porpoising foil are studied. Normally, it is possible to consider six degrees of freedom but in most cases, for practical applications, some degrees of freedom must be fixed. Here, pitch and heave are forced as sinusoidal functions $\frac{\pi}{2}$-dephased (see figure 3). Only the advance speed is not fixed. Since the motion generates thrust, the foil accelerates until he reaches a speed limit (see figure 4) when thrust and drag are at equilibrium. Its value depends on the characteristics of the motion like the heave amplitude h_0, the pitch amplitude δ_0, the frequency of the motion f_0, the foil span L and its chord c. When not enough thrust is produced, the foil is dragged backward by the current.

Let us apply the Buckingham theorem on this problem.

$$f(V_{lim}, h_0, \delta_0, f_0, L, c) = 0$$

These variables are reduced to two independent fundamental physical quantities: meter and second. Considering six variables, the f-expression is equivalent to an equation in-

volving a set of four dimensionless variables:

$$F(\frac{V_{lim}}{cf_0}, \frac{h_0}{c}, \delta_0, \frac{L}{c}) = 0$$

Two known dimensionless numbers appear: the Strouhal number $St = \frac{cf_0}{V_{lim}}$ and the wing aspect ratio $\Lambda = L/c$. We call $h_0^* = h_0/c$ the relative amplitude. Then:

$$F(St^{-1}, h_0^*, \delta_0, \Lambda) = 0 \tag{4}$$

The foil reaches its speed limit when it produces no more thrust in the advance direction. This behaviour is analogous to a propeller running idle. It is interesting to mention that all simulations tend to reach a limit velocity such as the Strouhal number is between 0.2 and 0.4 as for the fish and cetacean. In order to study the influence of the different dimensionless parameters on the hydrodynamic performances, the method used for a propeller is applied: the motion is forced, all the degrees of freedom are fixed and the input and output power are calculated.

3.3 Porpoising foil

Series of simulations have been launched with no degree of freedom. The aim is to compute the forces acting on the foil in order to understand the influence of the different parameters on the hydrodynamic performances, leading to the most efficient motion. The efficiency is defined, according to Anderson et al. (1998), as the ratio of the average of the output and the input power over a period. Hydrodynamic forces acting on the foil are the heave force $Y(t)$ and the torque $Q(t)$. The output force is represented by the thrust produced in the advance direction $X(t)$. Thus, the average input power is:

$$P = \frac{1}{T}\int_0^T (Y \times \dot{y} + Q \times \dot{\delta})dt \tag{5}$$

with T, the period of the motion, and the average output power is:

$$FU = \frac{U}{T}\int_0^T X dt \tag{6}$$

So, the efficiency of the porpoising motion is defined as:

$$\eta = \frac{FU}{P} \tag{7}$$

C_{Th} is then defined as:

$$C_{Th} = \frac{F}{\frac{1}{2}\rho S U^2} \tag{8}$$

A simulation corresponds to a number of Strouhal for a heave and a pitch amplitudes. Only the frequency of the motion is changed between two points on the same curve. Then the amplitudes are changed in order to obtain series of curves. This permits to understand the role of each parameter. In this section, the results for the thrust coefficient

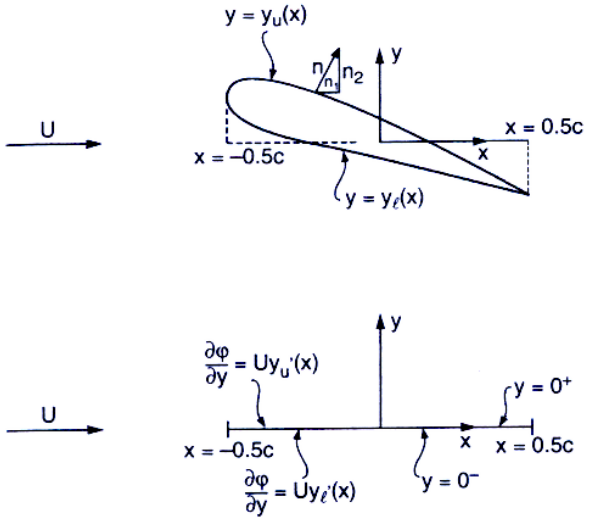

Figure 5: Linearization of boundary value problem of steady flow past a foil in infinite fluid. (top) Defines the foil geometry; (bottom) illustrates how body boundary conditions on the foil through linearization are transferred to a cut along the x-axis from $x = -c/2$ to $x = c/2$ with c the chord length.(Faltinsen, 2005)

C_{Th} are verified by comparing them with the analytical solution deduced from the Thoedorsen theory. This theory is detailed in Faltinsen (2005). Let us sum it up here.

First, we consider A 2D linear steady flow past a foil in infinite fluid. Linearity means that the fluid velocity $|\nabla\varphi|$ due to the foil is much smaller than the mean velocity U and that only linear terms in φ are kept in the formulation of the boundary value problem. We assume non-cavitating foil. We start by linearizing the body condition on the foil. The terminology used in the following is reported on figure 5. The exact body boundary condition on $y = y_u(x)$ is:

$$\frac{\partial\varphi}{\partial n} = -Un_x \tag{9}$$

with n_x, the x-component of the normal vector.

We can write $\frac{\partial\varphi}{\partial n} = n_x\frac{\partial\varphi}{\partial x} + n_y\frac{\partial\varphi}{\partial y}$. Because $n_x << n_y$ on the most part of the foil surface, we write $\frac{\partial\varphi}{\partial n} \sim \frac{\partial\varphi}{\partial y}$ on $y = y_u(x)$. The next step is to obtain the Taylor series of this boundary condition about $y = 0^+$ that is:

$$\frac{\partial\varphi}{\partial y} = \left.\frac{\partial\varphi}{\partial y}\right|_{y=0^+} + y_u\left.\frac{\partial^2\varphi}{\partial y^2}\right|_{y=0^+} + ...$$

for $-c/2 < x < c/2$ and because y_u is small, we take $\frac{\partial\varphi}{\partial y} = Uy_u'$ on $y = y_0^+$ (similarly for the lower part).

Next, the flow is separated into two parts that are respectively antisymmetric and symmetric about the x-axis. We then define the mean camber line of the foil: $\eta = 0.5(y_u(x) + y_l(x))$ and $y_u(x) = \eta(x) + a(x)$ and $y_l(x) = \eta(x) - a(x)$, then $\frac{\partial\varphi}{\partial y} = U[\eta'(x) \pm a'(x)]$ on $y = 0^{\pm}$.

We introduce the decomposition $\varphi = \varphi_0 + \varphi_e$, then $\frac{\partial \varphi_0}{\partial n} = U\eta'(x)$ on $y = 0$ and $\frac{\partial \varphi_e}{\partial n} = \pm Ua'$ on $y = 0^{\pm}$. The solution was for a steady foil. For the unsteady lifting problem, the linearised body boundary condition must be modified by accounting for the relative vertical velocity $V_R(x,t)$ between the foil and the incident foil. On $y = 0$ and for $-c/2 < x < c/2$,

$$\frac{\partial \varphi}{\partial y} = V_R(x,t) + U\eta'(x,t)$$

The total velocity potential is $Ux + \varphi$.
Now, we consider a 2D thin foil oscillating harmonically in heave and pitch. The vertical motion (heave) of the center of the foil is expressed as $h(t) = \Re\{h_0 e^{i\omega t}\}$ and the pitch angle is $\delta(t) = \Re\{i\delta_0 e^{i\omega t}\}$. The vertical motion of the mean camber line is $\eta = h - \delta x$. Then, on $y = 0$ and for $-c/2 < x < c/2$:

$$\frac{\partial \varphi}{\partial y} = V_R - U\frac{\partial \eta}{\partial x} = \dot{h} - \dot{\delta}x - U\delta \qquad (10)$$

Joukowsky condition (zero pressure jump across the free shear layer) on $y = 0$ and for $c/2 < x < c/2 + Ut$ (trailing edge) leads to:

$$\frac{\partial}{\partial t}(\varphi^+ - \varphi^-) + U\frac{\partial}{\partial x}(\varphi^+ - \varphi^-) = 0 \qquad (11)$$

The free shear layer can be represented in terms of a vortex distribution with density $\gamma(x,t)$ with $\frac{\partial \gamma}{\partial t} + U\frac{\partial \gamma}{\partial x}$ thus $\gamma(x,t) = \gamma(x - Ut)$. The vortex density in the wake has the mathematical form $\gamma = \Re\{\gamma_0 e^{i(\omega t - \frac{\omega}{Ux})}\}$. So the vortex density propagates as a sinusoidal wave with speed U along the x-axis. The wave number is ω/U which gives a wavelength of $2\pi U/\omega$. A complete solution is detailed in Theodorsen (1935). It follows that:

$$\begin{aligned} L = &- 0.25\rho\pi c^2(\ddot{h} - U\dot{\delta}) \\ &- \rho\pi U c C(k_f)(\dot{h} - U\delta - \frac{c\dot{\delta}}{4}) \end{aligned} \qquad (12)$$

with $k_f = \frac{\omega c}{2U}$ is the reduced frequency;

$$C(k_f) = F(k_f) + iG(k_f) = \frac{H_1^{(2)}(k_f)}{H_1^{(2)}(k_f) + iH_0^{(2)}(k_f)} \qquad (13)$$

with F and G are the real and imaginary parts of $C(k_f)$. $H_n^{(2)}$ are Hankel functions (Abramowitz, 1964) which can be expressed in terms of Bessel functions of the first and second kind, $H_n^{(2)} = J_n - iY_n$. $C(k_f)$ is called the Theodorsen function. When $\omega = 0$, $C(k_f)$ is equal to one so the well-known result for steady lifting problem is found i.e. $L = \rho\pi c U^2 \delta_0$.
The analytical C_{Th} is calculated from eq.(12). The numerical and analytical curves for three types of simulation (1- $h_0^* = 0.25$ and $\delta_0 = 15°$, 2- $h_0^* = 0.5$ and $\delta_0 = 15°$, 3- $h_0^* = 0.75$ and $\delta_0 = 10°$) are plotted on figure 6. The numerical and analytical results are comparable.

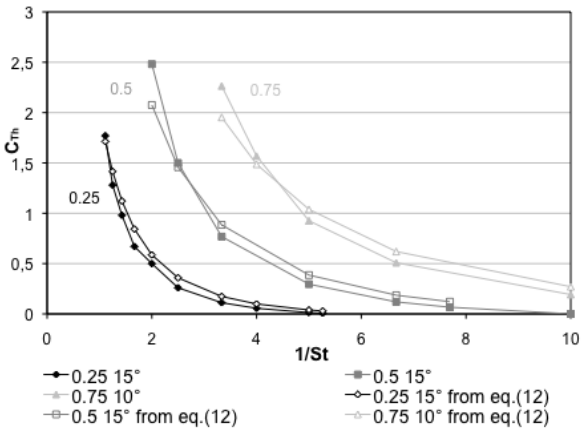

Figure 6: Comparison between the analytical and the numerical thrust coefficient for different h_0^* and δ_0

4 COMPARING FOIL VS PROPELLER

After this verificaton study, the aim is to compare the hydrodynamic performances of a porpoising foil and a high efficiency propeller.

4.1 Parameters

Dimensionless parameters must be defined to compare propeller and porpoising foil. A connection must be made between propeller and foil non-dimension parameters. Actually, the reference surface in the propeller case is the disk area which represents the obstruction made by the propeller in the current. In the porpoising foil case, the product of twice the heave amplitude by the wing length is a good approximation of the obstruction. The reference length used for the propeller is the diameter. The appropriate length in the foil case is thus the equivalent diameter of the obstruction area. So, curves for the porpoising foil are now plotted versus an equivalent advance parameter $J_{eq} = \frac{V}{f_0 D_{eq}}$ with $D_{eq} = \sqrt{\frac{8h_0 L}{\pi}}$.

4.2 Results

4.2.1 General

The influence of the different parameters on the hydrodynamic performances of the porpoising foil are first discussed. Then a comparison between a propeller and a porpoising foil is made.
The aspect ratio Λ is fixed equal to 10 in order to obtain a 2D problem to compare the hydrodynamic performances to the theory. Concerning the relative amplitude, as shown on figure 6 and 7, increasing h_0^* makes the curves shift to higher advance parameter J. It has an equivalent effect as increasing the relative pitch P/D Kuiper (1992). The pitch amplitude δ_0 has little effect on the coefficient C_{Th} (see figure 8). The effective angle of attack α_0 is calculated from the pitch and the heave amplitudes, the frequency of

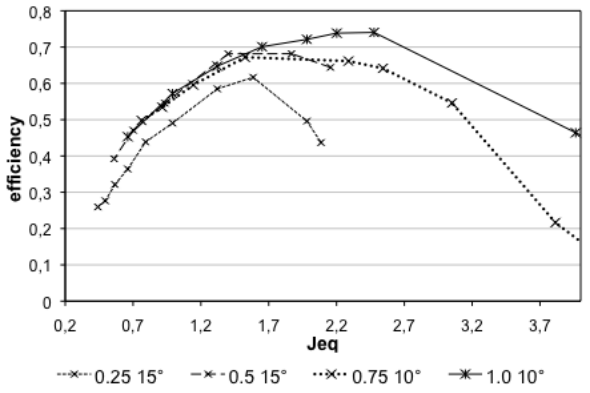

Figure 7: The porpoising foil efficiency η as defined in eq.(7) versus J_{eq} for different values of h_0^* and δ_0

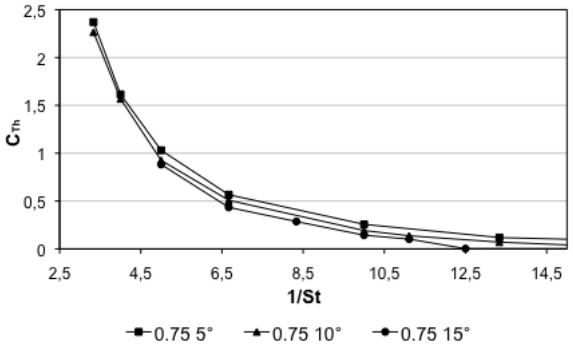

Figure 8: C_{Th} versus St^{-1} for a constant h_0 and different δ_0

the motion and the advance speed:

$$\alpha_0 = \arctan(\frac{-2\pi f_0 h_0}{U_\infty}) - \delta_0 \qquad (14)$$

The arctangent term dominates in this expression. h_0 has therefore more influence than δ_0 on the foil effective angle of attack α_0. In all our simulations, α_0 is little and h_0^* is ~ 1 which corresponds to a large pitch value for a propeller. In practical applications, the pitch is rarely taken greater than 1.5. In fact, to work with high pitch, a propeller needs to turn slowly which is not convenient with the actual motorization and the gear used. Besides, using little effective angle of attack permits to use a potential flow code because the separation of the boundary layer is avoided.

In the case of a propeller, on an efficiency curve, the pitch is taken constant which induces an effective angle of attack α_0 different for each value of J. In our simulations, to produce an efficiency curve, the amplitude h_0^* and the angle δ_0 are taken constant which is coherent with the propeller method in the limit of reasonable effective angle of attack α_0.

To concretise our comparison, a real high efficiency propeller is simulated (see figure 9). A propeller with a diameter of 5.5 m and a pitch of 0.8 is chosen. The thrust coefficient C_{Th} for a propeller is:

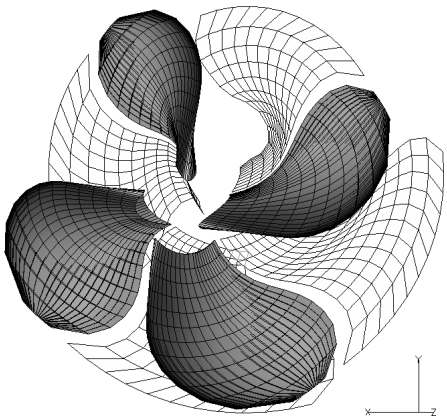

Figure 9: Panels of the propeller and its wake ($P/D = 2$)

$$C_{Th} = \frac{8D^2n^2K_T}{\pi U_\infty^2} \qquad (15)$$

with D the diameter of the propeller and n its number of rotation per second.

The maximum efficiency of the porpoising foil is obtained for higher J. According to the Wageningen B-series curves (Kuiper, 1992), simulations with the same propeller but with a higher pitch ($\simeq 2$) has been launched. As figures 10 and 11 show, the hydrodynamic performances of a fixed pitch-and-heave-amplitudes hydrofoil correspond to those of a fixed pitch propeller. The maximum efficiency for a pitch of 1.7 is obtained for the same advance parameter than for a foil motion of amplitudes $h_0^* = 0.25$ and $\delta_0 = 15°$. Their thrust coefficient curves are also corresponding. Thus the propeller with a pitch of 1.7 is comparable to the foil motion of amplitudes $h_0^* = 0.25$ and $\delta_0 = 15°$. Similarly, the propeller with a pitch of 2.7 is comparable to the foil motion of $h_0^* = 0.5$ and $\delta_0 = 15°$. Therefore, changing the pitch of a propeller has the same effect than changing the heave and pitch amplitudes, like a variable pitch propeller. Hence, heave and pitch amplitudes have to be considered as geometric parameters. Changing the rotational speed of the propeller corresponds to a change of frequency for the foil motion. For instance, a cycloidal propeller changes the frequency of its motion to accelerate. Its advance parameter J changes. Nevertheless its efficiency is calculated on one curve like a fixed pitch propeller. So the efficiency cannot be maximum for all speeds. When the angle between the foils of the cycloidal propeller and the current is modified, the purpose is to change the direction of the motion and not to modify the advance parameter. To jump from one efficiency curve to another, the cycloidal propeller would need to change its diameter in time. Inversely, a variable pitch propeller conserves its efficiency maximum for each J.

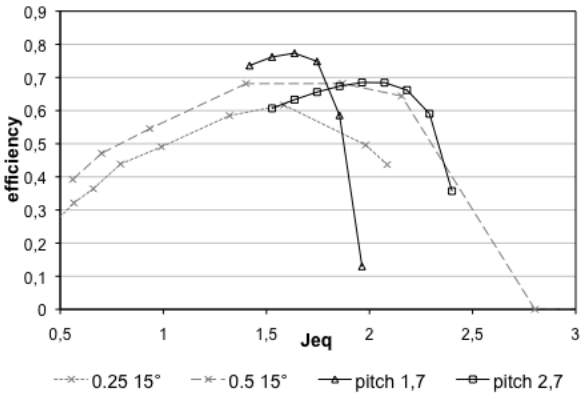

Figure 10: Efficiency of a porpoising foil with different h_0^* and δ_0 and a propeller with different pitch values

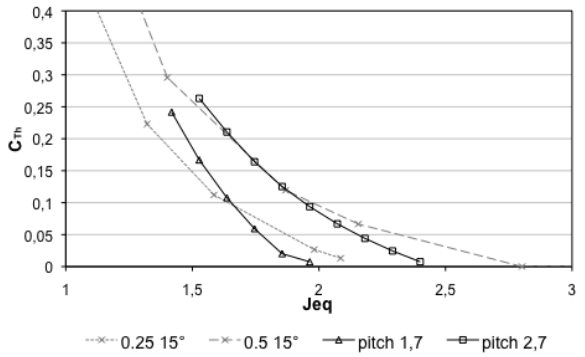

Figure 11: Thrust coefficient of a porpoising foil with different h_0^* and δ_0 and a propeller with different pitch values

In the following paragraph, a comparison is realized between the performance of a variable pitch propeller and a variable pitch-and-heave-amplitudes hydrofoil.

4.2.2 variable pitch

In order to simulate a variable pitch propeller, we use an initial mesh of the propeller with an initial pitch. Then, the angular velocity around the axis of the blade is embedded in the routine and the mesh is transformed at each time step to represent the blade with its new pitch. Thus, at each time step, the sources and doublet distributions have to be recalculated. This induces a simulation time more important than with a fixed pitch propeller, steady state simulation.The wake being generated in a lagrangian manner, the result takes into account for the position change. Moreover, the advance velocity is changed at each time step in order to be at the maximum efficiency for each pitch value. That is what happened on a boat equiped with a variable pitch propeller: when the speed changes, the pitch is adapted. The same procedure is used for the foil. At each time step, the code provides us the J, K_T, K_Q and η. So each time step represents a point on the graph. Inversely for the foil, to obtain C_{Th}, C_Q and η, an average is made over a period. So the number of points depends on the number of periods the foil needs to change its motion. The faster it changes, the fewer points there are, and the lower the efficiency is. On figure 12, efficiency is represented with the heave position of the foil. When the motion changes between two uniform motions, an hybrid motion appears, less efficient than the uniform one.

As expected, the efficiency of the variable pitch propeller is always maximum between two positions (different pitch, different advance parameters). The efficiency of a fixed pitch propeller follows a single curve. A change in J implies a η change restricted to one curve. In the hydrofoil case, the performances being calculated over a period, the change of motion is not continuous and the efficiency pass by a minimum between the two stable positions. The efficiency curves obtained for a fixed and a variable pitch propeller and a fixed and a variable pitch-and-heave-amplitudes porpoising foil are grouped together on the figure 13.

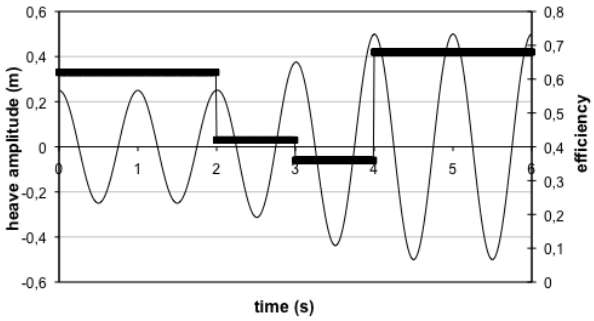

Figure 12: Change of the heave amplitude of a porpoising foil and the corresponding efficiency

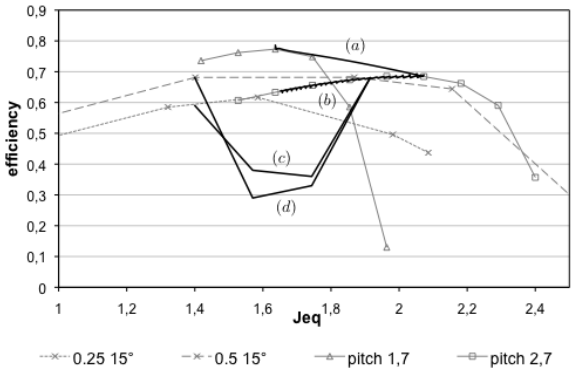

Figure 13: Comparison of efficiency of a change in the advance parameter J_{eq} for: (a) a variable pitch propeller; (b) a fixed pitch propeller; (c) a porpoising foil with variable pitch-and-heave-amplitudes and (d) a fixed pitch-and-heave-amplitudes porpoising foil. (Grey curves are presented for information about the departure and the arrival points of the J_{eq} variation)

5 CONCLUSION AND FUTURE WORK

We have presented numerical studies about porpoising hydrofoils and propellers. The thrust coefficient obtained for the foil is coherent with the analytical results deduced from the Theodorsen theory. Then, the influence of the important dimensionless parameters of the problem on the hydrodynamic performances is studied. Only the aspect ratio is fixed large enough to compare the results to the 2D theory. Heave and pitch amplitudes are geometric parameters. The combination of both has the same influence as the pitch for a propeller. It would be interesting to build an experiment with a prototype of an hydrofoil with variable pitch and heave amplitudes in order to validate our results.

Another study is in progress. This unsteady potential code permits also to simulate an hydrofoil with a camber changing in time. To realize such simuations, meshes for different curves are recorded in advance. Then, the routine calls at each time step the new mesh and recalculates the sources and doublets distributions. The camber of the foil induces different effective angle of attack, and this coupled with a heave motion could replace the porpoising motion.

Finally, the computational procedure also allows for several foils. We also plan to study the hydrodynamic performances of antisymmetrical twin foils propulsion.

ACKNOWLEDGMENT

This work is supported by the Délégation Générale pour l'Armement.

REFERENCES

Abbott, I. H. and Von Doenhoff, A. E. (1959). Theory of wing sections. Dover Publications, Inc. - New York.

Abramowitz, M. (1964). Handbook of mathematical functions. Applied Mathematics Series.

Anderson, J., Streitlien, K., Barrett, D., and Triantafyllou, M. (1998). Oscillating foils of high propulsive efficiency. JFM, 360:41–72.

Barrett, D., Triantafyllou, M., Yue, D., Grosenbaugh, M., and Wolfgang, M. (1999). Drag reduction in fish-like locomotion. JFM, 392:183–212.

Faltinsen, O. M. (2005). Hydrodynamics of high-speed marine vehicles. Cambridge university press.

Floc'h, F., Laurens, J.-M., Leroux, J. B., and Kerampran, S. (2008). Trajectory prediction by coupling euler-newton equations and flow models. In 11th Numerical Towing Tank Symposium, Brest, France.

Guglielmini, L. and Blondeaux, P. (2004). Propulsive efficiency of oscillating foils. European Journal of Mechanics B/Fluids, 23:255–278.

Guglielmini, L., Blondeaux, P., and Vittori, G. (2004). A simple model of propulsive oscillating foils. Ocean Engineering, 31:883–899.

Hoeijmakers, H. (1991). Panel methods for aerodynamic analysis and design. AGARD Report R-783.

Jurgens, D. (2001). Cycloidal rudders and propulsors. In 36th WEGEMT summer school, Rome, Italy.

Kuiper, G. (1992). The Wageningen propeller series. MARIN Publication.

Pedro, G., Suleman, A., and Djilali, N. (2003). A numerical study of the propulsive efficiency of a flapping hydrofoil. IJNMF, 42:493–526.

Schouveiler, L., Hover, F., and Triantafyllou, M. (2005). Performance of flapping foil propulsion. JFS, 20:949–959.

Streitlien, K., Triantafyllou, G., and Triantafyllou, M. (1996). Efficient foil propulsion through vortex control. AIAA Journal, 34(11):2315–2319.

Theodorsen, T. (1935). General theory of aerodynamic instability and the mechanism of flutter. NACA report, 496.

Triantafyllou, M., Triantafyllou, G., and Yue, D. (2000). Hydrodynamics of fishlike swimming. ARFM, 32:33–53.